Robust UAV Communications with Jamming

Haichao Wang[1](✉), Junnan Yao[1], Jin Chen[1], Guoru Ding[1,2], and Ling Yu[1]

[1] Army Engineering University, Nanjing 210007, China
whcwl0919@sina.com, tms3216@163.com, chenjin99@263.net,
dr.guoru.ding@ieee.org, yl2811284434@126.com
[2] Southeast University, Nanjing 210096, China

Abstract. Unmanned aerial vehicle (UAV) communication has attracted increasing attention recently, benefiting from its high mobility. However, most existing studies concentrate on a perfect scenario, without considering the unintentional interference/intentional jamming and uncertain channel/location information. In addition, the UAV-to-UAV (U2U) communication scenario has not been widely investigated as the UAV-to-Ground case. To fill this gap, this paper investigates the robust U2U communications in the presence of jamming, where the U2U communication channel and jammer location are considered to be uncertain, i.e., only having partial information. For the non-convex optimization with the aim of minimizing the flight time, we propose a successive convex approximation method by introducing S-procedure and slack variables. The inner optimization is transformed into a semidefinite programming problem, which can be optimally solved by standard convex techniques. Simulation results validate the proposed path planning method in the presence of jamming.

Keywords: Unmanned aerial vehicle · Jamming · Path planning · Robust optimization

1 Introduction

The high-data rate and low-delay requirements for wireless communications pose a critical threat to the existing terrestrial communication system with limited network resource. To this end, many aerial/space communication platforms, such as unmanned aerial vehicles (UAVs) and satellites, have been leveraged to provide better service for terrestrial users, which forms a widely known Space-Air-Ground Integrated Network (SAGIN).

UAV, as one of critical elements in SAGIN, has been attracted increasing attentions in wireless communications due to its wide applications [1–3], such as aerial base station [4–6], relay [7–10], energy source [11,12], etc. Specifically, authors in [1] proposes a surveillance system for amateur UAVs based on cognitive internet of things. UAV' potentials in wireless communications versus

M. Jia et al. (Eds.): WiSATS 2019, LNICST 280, pp. 104–116, 2019.
https://doi.org/10.1007/978-3-030-19153-5_10

traditional fixed infrastructure based communications have been studied in [2]. Furthermore, authors in [3] show its advantages in communications, caching, and energy transfer. As aerial base stations [4–6], they embody a three-dimensional (3D) characteristic, where the UAV altitude has an important impact on the system performance. The reason is that, in general, increasing the UAV altitude results in a higher path-loss, but it also improves the probability of having line-of-sight (LoS) link. The optimal altitude for both static and mobile UAVs as relays has been investigated in [7]. In [8], a joint 3D location and transmit power optimization problem in a UAV relaying network with multiple mobile users is studied. On the other hand, authors in [8–10] utilized the UAV horizontal mobility to improve the terrestrial network performance. In addition, UAV-enabled wireless power transfer has been investigated in [11,12] for mobile case and static case, respectively.

The aforementioned studies focus on a perfect scenario, i.e., no interference and jamming signals. In practice, UAV communications may experience jamming, however, with few researches. In this paper, we study the robust UAV-to-UAV (U2U) communications in the presence of jamming. Specifically, the contributions of this paper are summarized as follows:

– We formulate a path planning problem for U2U communications in the presence of jamming, which considers the air-to-air channel uncertainty, jammer location uncertainty, UAV maximum flight speed, and the signal-to-interference-plus-noise-ratio (SINR) requirement. The aim is to minimize the flight time via designing the UAV path.
– We develop a path planning algorithm with the aid of S-procedure, successive convex approximation (SCA), and semidefinite programming (SDP). In particular, the probability constraint is firstly transformed into a tractable equivalence by introducing the slack variables and S-procedure. Then, the SCA is leveraged to tackle the determined optimization problem, where SDP is embedded.

The rest of this paper is organized as follows. In Sect. 2, we illustrate the investigated scenario and formulate the optimization problem. Then, we design a path planning method in Sect. 3 by leveraging the SCA and SDP. Simulation results are presented to verify the effectiveness of the proposed approach in Sect. 4. Finally, we conclude this paper in Sect. 5.

2 System Model and Problem Formulation

2.1 System Model

Consider two UAVs cooperatively perform a series of tasks and exchange information while flying in the air. As an example, two mobile UAVs aim to share the transport and surveillance information collected by the ground sensors in vehicle networks. Meanwhile, a set of terrestrial jammers, denoted as the set $\mathcal{M}$, attacks the UAV communications, as shown in Fig. 1. To enable efficient communications, UAVs maintain a small distance during the flight. Since the distance between UAVs is much smaller than the space of interest and the distances between UAVs and jammers, their positions ($\mathbf{w}_1$ and $\mathbf{w}_2$) are approximated by the coordinate $\mathbf{w} = \{x, y, H\}$, measured in meters. The term $\{x, y\}$ represents the UAV horizontal position, whereas H indicates the UAV altitude. The UAV positions for performing current and next tasks are denoted as the start and end locations, respectively, represented by $\mathbf{w}^{\text{start}}$ and $\mathbf{w}^{\text{end}}$. Let T denote the time length which UAVs speed flying away to the end location from the start location. At any time instant $t \in [0, T]$, the UAV location is given as $\mathbf{w}(t) = \{x(t), y(t), H\}$. The total time length is discretized into N time slot, with each of $T[n]$ length [13]. The UAV location is $\mathbf{w}[n] = \{x[n], y[n], H\}$ at the n-th time slot. Thus, the UAV path $\{\mathbf{w}[n]\}_{n=0}^{n=N}$ is discretized into N line segment, and $\mathbf{w}[0] = \mathbf{w}^{\text{start}}, \mathbf{w}[N] = \mathbf{w}^{\text{end}}$. To ensure an almost continuous path, the length of each line segment is limited by $\Delta_{\max}$:

$$\|\mathbf{w}[n] - \mathbf{w}[n-1]\| \leq \Delta_{\max}, \forall n, \tag{1}$$

where $\Delta_{\max}$ is the maximum length of line segment.

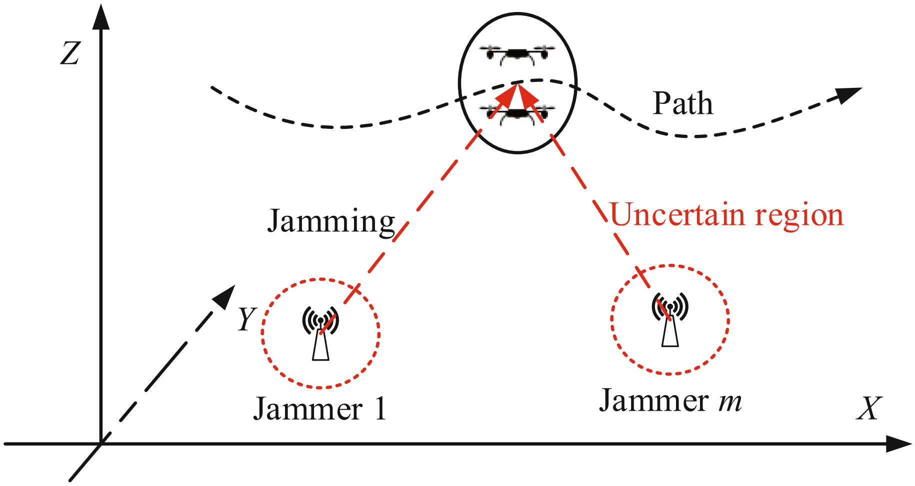

Fig. 1. Considered UAV-to-UAV communication scenario in the presence of jammers.

Based on the network state information, a ground node is responsible of planning UAVs behaviors, including altitude, velocity, etc. However, only partial information can be mastered by the ground node. Specifically, the UAVs parameters have been acquired. Due to the lack of cooperation between ground node and jammers, jammers locations cannot be acquired accurately. The errors between the exact location $\mathbf{w}_m^J = \{x_m^J, y_m^J, 0\}$ and estimated location $\bar{\mathbf{w}}_m^J = \{\bar{x}_m^J, \bar{y}_m^J, 0\}$

of m-th jammer is $\Delta \mathbf{w}_m^J = \mathbf{w}_m^J - \bar{\mathbf{w}}_m^J = \left\{\Delta x_m^J, \Delta y_m^J, 0\right\}$, and $\Delta \mathbf{w}_m^J$ is given by

$$\Delta \mathbf{w}_m^J \in \mathcal{U}_m = \left\{\left(\Delta x_m^J\right)^2 + \left(\Delta y_m^J\right)^2 \leq (L_m)^2\right\}. \tag{2}$$

Therefore, for a terrestrial jammer, it locates in a circular region with the estimated location $\bar{\mathbf{w}}_m^J$ as center and L_m as radius. Notably, the uncertain region may be irregular, but there is always a circle containing the irregular region. Thus, the studied uncertain region actually provides a conservative estimation for other irregular form.

The U2U (air-to-air) channel power gain g_u is modeled by average channel power gain along with a random variable accounting for the fading component, i.e.,

$$g_u = \beta_0 d_u^{-\alpha} \xi, \tag{3}$$

where β_0 is the channel power gain at the reference distance d_0, d_u is the distance between UAVs of interest, α is the path loss exponent, and ξ represents the fading and small scale effect. Since the air-to-air channel consists of dominant LoS link and non-dominant NLoS link, respectively, the Rice distribution is used to account for the small scale effect ξ and is given as [14,15]

$$f\left(\xi \middle| \rho, \mu\right) = \frac{\xi}{\rho^2} \exp\left(-\frac{\xi^2 + \mu^2}{2\rho^2}\right) I_0\left(\frac{\xi\mu}{\rho^2}\right), \tag{4}$$

with $\xi \geq 0$, where $I_0(x)$ is the modified Bessel function of the first kind with order zero, and ρ and μ reflecting the strength of the scattered (non-dominant) and dominant paths. It can be observed that Rice channel model reduces to a Rayleigh model when there is no dominant signal $\mu = 0$, i.e., $f\left(\xi \middle| \rho\right) = \frac{\xi}{\rho^2} \exp\left(-\frac{\xi^2}{2\rho^2}\right)$.

The channel of the interference link from the m-th jammer to the UAV is dominated by LoS transmission [9],

$$g_m^J[n] = \beta_0 \left\|\mathbf{w}[n] - \mathbf{w}_m^J\right\|^{-\alpha} = \beta_0 \left\|\mathbf{w}[n] - \bar{\mathbf{w}}_m^J - \Delta \mathbf{w}_m^J\right\|^{-\alpha}, \forall m \in \mathcal{M}, \tag{5}$$

at the n-th line segment, where $\|\mathbf{a}\|$ provides the Euclidean norm for vector $\mathbf{a}$. Notably, $g_m^J[n]$ is not perfectly known since we only have partial information on $\Delta \mathbf{w}_m^J$. It can be observed that the location uncertainty is finally mapped to the channel state. Thus, the studied location uncertainty can be understood from different perspectives. On one hand, it initially characterizes the location uncertainty. Besides, it can be also regarded as the CSI uncertainty, which results from the random small scale fading or estimation errors.

2.2 Problem Formulation

The received SINR at the n-th line segment is given by

$$SINR[n] = \frac{P_u g_u}{\sum_{m=1}^{M} P_m^J[n] g_m^J[n] + \sigma^2}, \tag{6}$$

where P_u is the transmit power of UAV-Tx, P_m^J is the jammer power of m-th jammer, σ^2 is the noise power, and unit bandwidth is considered. Since future jammer power $P_m^J[n]$ cannot be acquired accurately, average jammer power is used in this paper and considered to be known. Then, the received SINR in the worst case is

$$\min_{\{\Delta \mathbf{w}_m^J\}} SINR[n] = \frac{P_u g_u}{\max\limits_{\{\Delta \mathbf{w}_m^J\}} \sum_{m=1}^{M} P_m^J[n]\, g_m^J[n] + \sigma^2}. \tag{7}$$

To ensure the U2U communication, the outage probability in the worst case is limited as follows:

$$\Pr\left[\min_{\{\Delta \mathbf{w}_m^J\}} SINR[n] \le \gamma_{th}\right] \le \varepsilon, \forall n, \tag{8}$$

where $\Pr[A]$ represents the occurrence probability of an event A, γ_{th} is the required SINR, ε is maximum allowable outage probability, and "min" makes it still work in the worst case since the jammers locations are uncertain.

In addition to the communication constraint, there is maximum flight speed on UAV. UAV path is limited by UAV maximum flight speed, i.e.,

$$\|\mathbf{w}[n] - \mathbf{w}[n-1]\| \le V_{\max} T[n], \forall n, \tag{9}$$

where $V_{\max}$ is the maximum speed.

The aim of this paper is to minimize the completion time T, i.e., flying toward the end location as soon as possible, by designing UAV path. The problem can be formulated as follows:

$$\begin{aligned}
(P1):\ & \min_{\{\mathbf{w}[n], T[n]\}} \sum_{n=1}^{N} T[n] \\
s.t.\ C1:\ & \Pr\left[\min_{\{\Delta \mathbf{w}_m^J\}} SINR[n] \le \gamma_{th}\right] \le \varepsilon, \forall n, \\
C2:\ & \|\mathbf{w}[n] - \mathbf{w}[n-1]\| \le \Delta_{\max}, \forall n, \\
C3:\ & \|\mathbf{w}[n] - \mathbf{w}[n-1]\| \le V_{\max} T[n], \forall n,
\end{aligned} \tag{10}$$

where $C1$ is outage probability constraint, $C2$ and $C3$ are the path constraints.

3 Time Minimization Algorithm for Robust UAV Communications

In $(P1)$, the probability constraints $C1$ is non-convex although there is a linear objective, and thus $(P1)$ cannot be efficiently solved by existing standard convex optimization methods.

Denote

$$I[n] = \max_{\{\Delta \mathbf{w}_m^J\}} \sum_{m=1}^{M} P_m^J[n]\, g_m^J[n] + \sigma^2. \tag{11}$$

Algorithm 1. One-dimensional search for obtaining parameter b

1: Initialize the parameters b^s, Δb, and set $s = 0$
2: **Repeat**
3: Update $b^s \leftarrow b^s + \Delta b$
4: Update $s \leftarrow s + 1$
5: **Until** $Q_1(a, b^s) < \varepsilon$
6: Output b^s

Then, the constraint in $C1$ can be rewritten as follows:

$$\Pr\left[\xi \leq \frac{I[n]\, d_u^{\alpha} \gamma_{th}}{P_u \beta_0}\right] \leq \varepsilon, \forall n. \tag{12}$$

Since random variable ξ follows Rice distribution, its cumulative distribution function (CDF) is given as standard Marcum Q-function $Q_1(a, b)$

$$Q_1(a, b) = \int_b^{\infty} x \exp\left(-\frac{x^2 + a^2}{2}\right) I_0(ax) dx. \tag{13}$$

Then, there is

$$\Pr\left[\xi \leq \frac{I[n]\, d_u^{\alpha} \gamma_{th}}{P_u \beta_0}\right] = 1 - Q_1\left(\frac{\mu}{\rho}, \frac{1}{\rho} \bullet \frac{I[n]\, d_u^{\alpha} \gamma_{th}}{P_u \beta_0}\right) \leq \varepsilon. \tag{14}$$

The standard Marcum Q-function $Q_1(a, b)$ is nondecreasing with respect to a and non-increasing with respect to b. Thus, given parameter a and probability ε, the parameter b can be obtained via one-dimensional search, denoted as $b = Q_1^{-1}(a, \varepsilon)$ [16]. Algorithm 1 provides the procedure for obtaining b with a given a and probability ε.

Now, the constraint in (14) can be rewritten as

$$\frac{I[n]\, d_u^{\alpha} \gamma_{th}}{P_u \beta_0} \leq \rho Q_1^{-1}\left(\frac{\mu}{\rho}, 1 - \varepsilon\right), \forall n, \tag{15}$$

or the following intractable form:

$$I[n]\, d_u^{\alpha} \gamma_{th} \leq \rho \beta_0 Q_1^{-1}(\mu/\rho, 1 - \varepsilon) P_u, \forall n. \tag{16}$$

Since the interference from each jammer is independent, there is

$$\begin{aligned} I[n] &= \max_{\{\Delta \mathbf{w}_m^J\}} \sum_{m=1}^{M} P_m^J[n]\, \beta_0 \left\| \mathbf{w}[n] - \bar{\mathbf{w}}_m^J - \Delta \mathbf{w}_m^J \right\|^{-\alpha} + \sigma^2 \\ &= \sum_{m=1}^{M} \frac{P_m^J[n]\, \beta_0}{\min\limits_{\Delta \mathbf{w}_m^J} \left\| \mathbf{w}[n] - \bar{\mathbf{w}}_m^J - \Delta \mathbf{w}_m^J \right\|^{\alpha}} + \sigma^2, \forall n. \end{aligned} \tag{17}$$

Introducing additional variable $\{U_m[n]\}$, the constraint in (16) can be replaced with

$$\left(\sum_{m=1}^{M} P_m^J[n]\,\beta_0 U_m^{-\alpha/2}[n] + \sigma^2\right) d_u^\alpha \gamma_{th} \le \rho\beta_0 Q_1^{-1}(\mu/\rho, 1-\varepsilon)\,P_u, \forall n, \tag{18}$$

$$U_m[n] \le \min_{\Delta\mathbf{w}_m^J} \left\|\mathbf{w}[n] - \bar{\mathbf{w}}_m^J - \Delta\mathbf{w}_m^J\right\|^2, \forall m, n \tag{19}$$

The Eq. (19) can be rewritten as

$$\left(\Delta x_m^J\right)^2 + \left(\Delta y_m^J\right)^2 \le L_m^2, \forall m \in \mathcal{M}, \tag{20}$$

$$U_m[n] \le \left(x[n] - \bar{x}_m^J - \Delta x_m^J\right)^2 + \left(y[n] - \bar{y}_m^J - \Delta y_m^J\right)^2 + H^2, \forall m \in \mathcal{M}, n, \tag{21}$$

The constraints in (20) and (21) are intractable to be addressed since there is infinite number of parameters $\left\{\Delta x_m^J, \Delta y_m^J\right\}$. To this end, we resort to the S-Procedure defined as follows [17]:

S-Procedure: Denote $\mathbf{F}_i$, $\mathbf{g}_i$, and h_i as the $n \times n$ symmetric matrix, n dimensional column vector, and real number, respectively. Then, the implication

$$\mathbf{x}^T\mathbf{F}_1\mathbf{x} + 2\mathbf{g}_1^T\mathbf{x} + h_1 \le 0 \Rightarrow \mathbf{x}^T\mathbf{F}_2\mathbf{x} + 2\mathbf{g}_2^T\mathbf{x} + h_2 \le 0, \tag{22}$$

holds if and only if there is a $\lambda \ge 0$ such that

$$\begin{bmatrix} \mathbf{F}_2 & \mathbf{g}_2 \\ \mathbf{g}_2^T & h_2 \end{bmatrix} \preceq \lambda \begin{bmatrix} \mathbf{F}_1 & \mathbf{g}_1 \\ \mathbf{g}_1^T & h_1 \end{bmatrix} \tag{23}$$

provided there exists a point $\bar{\mathbf{x}}$ with $\bar{\mathbf{x}}^T\mathbf{F}_1\bar{\mathbf{x}} + 2\mathbf{g}_1^T\bar{\mathbf{x}} + h_1 < 0$.

In the sequel, we address the constraints (20) and (21). It can be observed that $\left(\Delta x_m^J\right)^2 + \left(\Delta y_m^J\right)^2 - L_m^2 < 0$ with $\left(\Delta x_m^J, \Delta y_m^J\right) = (0,0)$. Based on the S-Procedure, (20) implies (21) if and only if

$$\varGamma\left(x[n], y[n], U_m[n], \lambda_m[n]\right) \succeq 0, \forall m \in \mathcal{M}, n, \tag{24}$$

where

$$\varGamma\left(x[n], y[n], U_m[n], \lambda_m[n]\right) = \begin{bmatrix} \lambda_m[n]+1 & 0 & \bar{x}_m^J - x[n] \\ 0 & \lambda_m[n]+1 & \bar{y}_m^J - y[n] \\ \bar{x}_m^J - x[n] & \bar{y}_m^J - y[n] & \varphi_m[n] \end{bmatrix} \tag{25}$$

with

$$\varphi_m[n] = -\lambda_m[n]\,L_m^2 + \left(x[n] - \bar{x}_m^J\right)^2 + \left(y[n] - \bar{y}_m^J\right)^2 - U_m[n] + H^2. \tag{26}$$

However, it is intractable to be addressed with the form in Eq. (24) since it results in a non-convex feasible region. Considering the fact that x^2 is convex, there is

$$\begin{aligned} x^2[n] &\ge -(x^s[n])^2 + 2x^s[n]\,x[n], \\ y^2[n] &\ge -(y^s[n])^2 + 2y^s[n]\,y[n]. \end{aligned} \tag{27}$$

Algorithm 2. Path planning for U2U communications with jamming

1: Initialize the parameters $P^s = \{\mathbf{w}[n], T[n], U_m[n], \lambda_m[n]\}$, and set $s = 0$
2: **Repeat**
3: Solve the SDP problem in (P2) with a feasible point P^s and find optimal solution P^*
4: Update $P^s \Leftarrow P^*$
5: Update $s \leftarrow s + 1$
6: **Until** the terminal condition is met
7: Output the path $P^* = \{\mathbf{w}[n], T[n]\}$

Therefore, Eq. (24) is lower bounded by the following linear matrix inequality (LMI):

$$\tilde{\varGamma}(x[n], y[n], U_m[n], \lambda_m[n]) = \begin{bmatrix} \lambda_m[n]+1 & 0 & \bar{x}_m^J - x[n] \\ 0 & \lambda_m[n]+1 & \bar{y}_m^J - y[n] \\ \bar{x}_m^J - x[n] & \bar{y}_m^J - y[n] & \tilde{\varphi}_m[n] \end{bmatrix} \tag{28}$$

with

$$\begin{aligned} \tilde{\varphi}_m[n] = & -\lambda_m[n] L_m^2 - (x^s[n])^2 + 2x^s[n]x[n] - (y^s[n])^2 \\ & + 2y^s[n]y[n] - 2\bar{x}_m^J x[n] - 2\bar{y}_m^J y[n] + \left(\bar{x}_m^J\right)^2 + \left(\bar{y}_m^J\right)^2 - U_m[n] + H^2. \end{aligned} \tag{29}$$

We should iteratively solve the following problems:

$$\begin{aligned} (P2): & \min_{\{\mathbf{w}[n], T[n], U_m[n], \lambda_m[n]\}} \sum_{n=1}^{N} T[n] \\ s.t.\ C1: & \begin{cases} \sum_{m=1}^{M} P_m^J[n] \beta_0 U_m^{-\alpha/2}[n] \le A, \forall n, \\ \tilde{\varGamma}(x[n], y[n], U_m[n], \lambda_m[n]) \succeq \mathbf{0}, \forall m, n, \\ \lambda_m[n] \ge 0, \forall m, n, \end{cases} \\ & C2: \|\mathbf{w}[n] - \mathbf{w}[n-1]\| \le \varDelta_{\max}, \forall n, \\ & C3: \|\mathbf{w}[n] - \mathbf{w}[n-1]\| \le V_{\max} T[n], \forall n, \end{aligned} \tag{30}$$

where $A = \frac{\rho \beta_0 Q_1^{-1}(\mu/\rho, 1-\varepsilon) P_u}{d_u^\alpha \gamma_{th}} - \sigma^2$. The $P2$ is a semidefinite programming (SDP) and can be solved by convex optimization techniques.

Finally, the algorithm to solve (P1) is summarized in Algorithm 2.

4 Simulations and Discussions

In this section, we illustrate the UAV behavior in the presence of jamming, and demonstrate the effectiveness of the proposed algorithm by conducting in-depth simulations. Consider a horizontal 1000×1000 m^2 scenario with two terrestrial jammers located at $(300, 300)$ and $(700, 700)$, respectively. Unless otherwise specified, the main simulation parameters are set as that listed in Table 1.

Table 1. Key parameters used in simulations.

Parameter	Value	Comments
P_m^J	0.5 W	Jammer power
β_0	−60 dB	Channel power gain at the reference distance d_0
ρ, μ	1.347, 6.469	The strength of the scattered and dominant paths
ε	0.1	Outage probability
P_u	0.1 W	UAV transmit power
d_u	20 m	Distance between UAVs
α	−3	The path loss exponent
γ_{th}	1	The required SINR
σ^2	−110 dBm	Noise power
$\Delta_{\max}$	100 m	The maximum length of line segment
$V_{\max}$	20 m/s	The UAV maximum flight speed
H	100 m	The UAV altitude
L_m	40 m	The uncertain radius

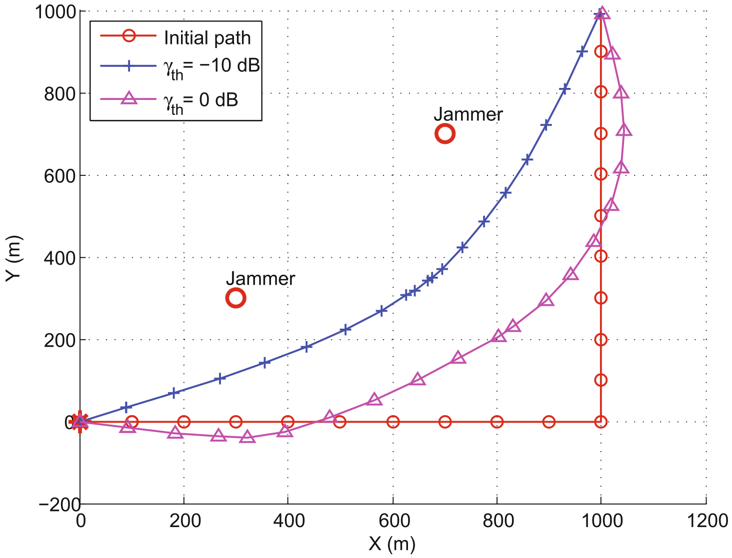

Fig. 2. UAV path in the presence of jammers with different considerations.

Figure 2 illustrates the UAV path in different considerations, where "$*$" and "$\circ$" represent the UAV start (end) location, jammer location, respectively. The initial path for start our algorithm has also been given in Fig. 2. It can be first observed that, in the presence of jamming, the UAV is intentionally far away

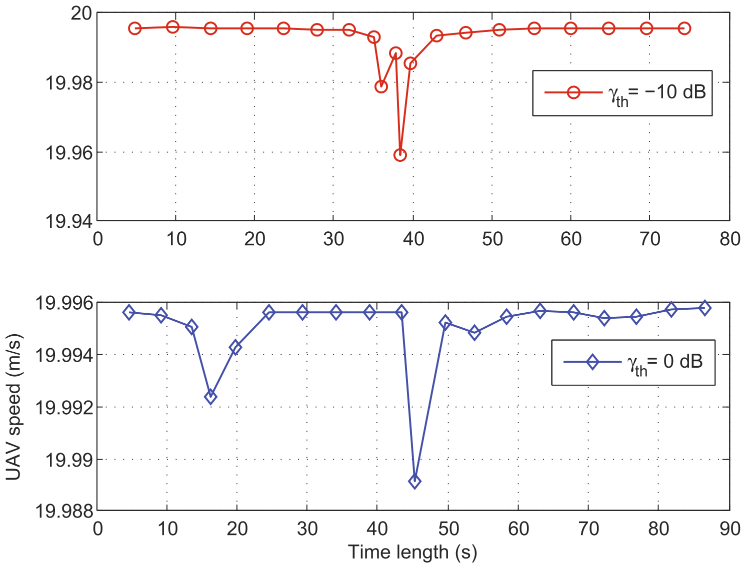

Fig. 3. UAV flight speed versus the time length.

from the jammer during the flight. Moreover, with higher SINR requirement, longer distance is required to avoid jamming.

To make the UAV path more intuitive, Fig. 3 presents the UAV speed versus the flight time, where the maximum flight speed is set to be 20 m/s. It can be found from Fig. 3 that the UAV passes through the jammer region at a maximum speed in all cases. This is expected since higher speed can save the flight time, without other considerations, such as the energy consumption.

The convergence behavior of the proposed path planning algorithm is plotted in Fig. 4. The time length consumed goes to a stable value after some iterations. Furthermore, it can be known from Fig. 2 that the initial path in the case of $\gamma = 0\,\text{dB}$ is not a feasible point. However, the proposed path planning algorithm can also achieve a feasible and high-performance solution, which is expected and proves the robustness of the algorithm.

Figure 5 plots the time length comparison versus the uncertain region with different SINR requirements. As expected, high uncertainty results in greater flight costs for the UAV. This is because the UAV must fly a longer distance to be away from jammers.

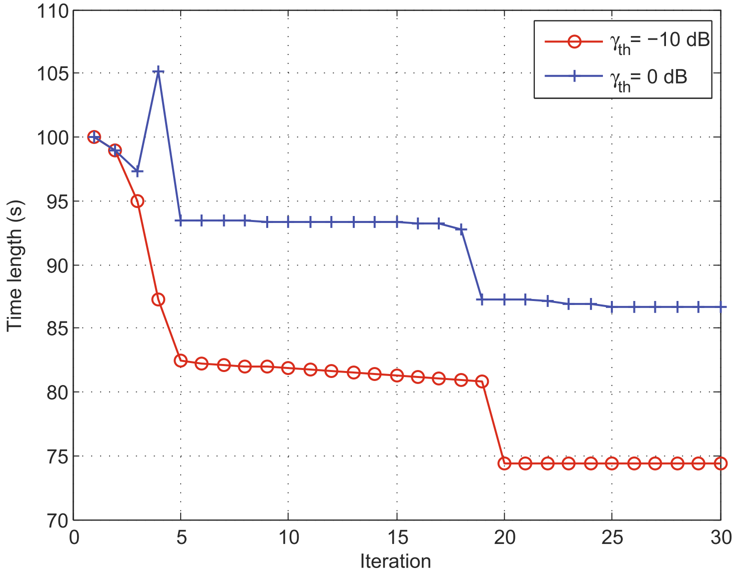

Fig. 4. The convergence behavior of the proposed path planning algorithm.

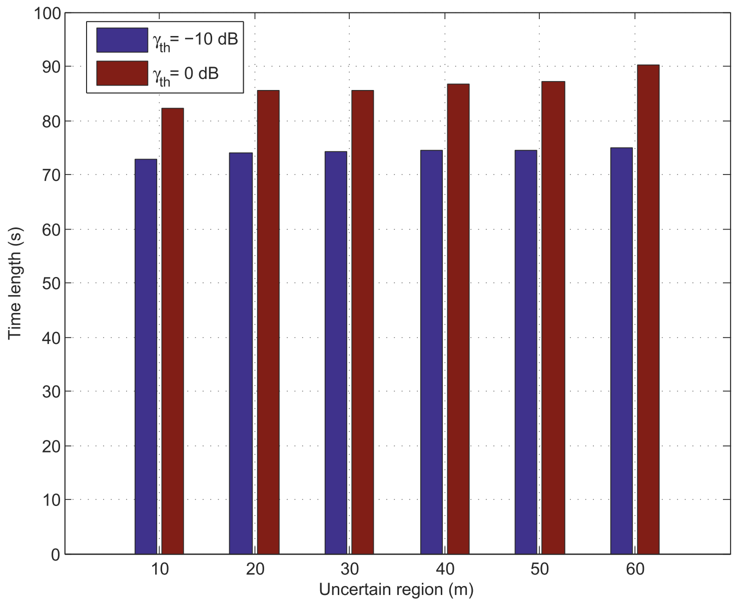

Fig. 5. Time length comparison versus the uncertain region with different SINR requirements.

5 Conclusions

UAVs have been attracted increasing attentions in wireless communications. In this paper, we studied the robust UAV communications in the presence of jamming. First, we formulated a path planning problem for U2U communications in the presence of jamming, which considered the air-to-air channel uncertainty, jammer location uncertainty, UAV maximum flight speed, and the SINR requirement. Then, we developed a path planning algorithm with the aid of S-procedure, successive convex approximation (SCA), and semidefinite programming (SDP). Simulation results validate the effectiveness of the proposed algorithm.

Acknowledgement. This work was supported in part by the National Natural Science Foundation of China under Grant 61871398 and Grant 61501510, and in part by the China Postdoctoral Science Foundation Funded Project under Grant 2018T110426.

References

1. Ding, G., Wu, Q., Zhang, L., Lin, Y., Tsiftsis, T.A., Yao, Y.D.: An amateur drone surveillance system based on the cognitive internet of things. IEEE Commun. Mag. **56**(1), 29–35 (2018)
2. Zeng, Y., Zhang, R., Teng, J.L.: Wireless communications with unmanned aerial vehicles: opportunities and challenges. IEEE Commun. Mag. **54**(5), 36–42 (2016)
3. Wang, H., Ding, G., Gao, F., Chen, J., Wang, J., Wang, L.: Power control in UAV-supported ultra dense networks: communications, caching, and energy transfer. IEEE Commun. Mag. **56**(6), 28–34 (2018)
4. Al-Hourani, A., Kandeepan, S., Lardner, S.: Optimal lap altitude for maximum coverage. IEEE Wirel. Commun. Lett. **3**(6), 569–572 (2014)
5. Alzenad, M., El-Keyi, A., Lagum, F., Yanikomeroglu, H.: 3-D placement of an unmanned aerial vehicle base station (UAV-BS) for energy-efficient maximal coverage. IEEE Wirel. Commun. Lett. **6**(4), 434–437 (2017)
6. Mozaffari, M., Saad, W., Bennis, M., Debbah, M.: Unmanned aerial vehicle with underlaid device-to-device communications: performance and tradeoffs. IEEE Trans. Wirel. Commun. **15**(6), 3949–3963 (2016)
7. Chen, Y., Feng, W., Zheng, G.: Optimum placement of UAV as relays. IEEE Commun. Lett. **22**(2), 248–251 (2018)
8. Xue, Z., Wang, J., Ding, G., Wu, Q.: Joint 3D location and power optimization for UAV-enabled relaying systems. IEEE Access **6**, 43113–43124 (2018)
9. Zeng, Y., Zhang, R., Teng, J.L.: Throughput maximization for UAV-enabled mobile relaying systems. IEEE Trans. Commun. **64**(12), 4983–4996 (2016)
10. Wang, H., Wang, J., Ding, G., Chen, J., Li, Y., Han, Z.: Spectrum sharing planning for full-duplex UAV relaying systems with underlaid D2D communications. IEEE J. Sel. Areas Commun. **36**(9), 1986–1999 (2018)
11. Xu, J., Zeng, Y., Zhang, R.: UAV-enabled wireless power transfer: trajectory design and energy optimization. IEEE Trans. Wirel. Commun. **17**(8), 5092–5106 (2018)
12. Wang, H., Wang, J., Ding, G., Wang, L., Tsiftsis, T.A., Sharma, P.K.: Resource allocation for energy harvesting-powered D2D communication underlaying UAV-assisted networks. IEEE Trans. Green Commun. Netw. **2**(1), 14–24 (2018)
13. Zeng, Y., Xu, J., Zhang, R.: Energy minimization for wireless communication with rotary-wing UAV (2018). http://cn.arxiv.org/pdf/1804.02238

14. Goddemeier, N., Wietfeld, C.: Investigation of air-to-air channel characteristics and a UAV specific extension to the Rice model. In: IEEE GLOBECOM Workshops, pp. 1–5. IEEE (2015)
15. Kim, M., Lee, J.: Outage probability of UAV communications in the presence of interference (2018). http://cn.arxiv.org/pdf/1806.09843.pdf
16. Zheng, G., Ma, S., Wong, K.K., Ng, T.S.: Robust beamforming in cognitive radio. IEEE Trans. Wirel. Commun. **9**(2), 570–576 (2010)
17. Boyd, S., Vandenberghe, L.: Convex Optimization. Cambridge University Press, Cambridge (2004)